Available online at www.sciencedirect.com
SCIENCE DIRECT®
Journal of Organometallic Chemistry 689 (2004) 1444–1451
Journal of Organometallic Chemistry
www.elsevier.com/locate/jorganchem

Chloride substitution of [CpRu(dppf)Cl] with sulfur-containing ligands

Xiu Lian Lu, Jagadese J. Vittal, Edward R.T. Tiekink, Lai Yoong Goh *, T.S. Andy Hor *

Department of Chemistry, National University of Singapore, 3 Science Drive 3, Kent Ridge, Singapore 117543, Singapore

Received 17 November 2003; accepted 15 December 2003

Abstract

The reactions of CpRu(dppf)Cl (**1**) with the sulfur-containing ligands, thiophenol HSPh, 2-mercaptopyridine $C_5H_4N(SH)$, thiourea $SC(NH_2)_2$, vinylene trithiocarbonate $SCS(CH)_2S$ and ethylene trithiocarbonate $SCS(CH_2)_2S$, yielded chloro-substituted derivatives, viz. the mono-ruthenium(II) complexes CpRu(dppf)(SPh) (**2**), $[CpRu(dppf)(SC_5H_4NH)]BPh_4$ (**3**)BPh_4, $[CpRu(dppf)(SC(NH_2)_2]PF_6$ (**4**)PF_6, [CpRu(dppf)(SCS(CH)$_2$S)]Cl (**5**)Cl and [CpRu(dppf)(SCS(CH$_2$)$_2$S)]Cl (**6**)Cl, respectively. Treatment of **1** with $AuCl(SMe_2)$ in the presence of NH_4PF_6 gave $[(CpRu(dppf)(SMe_2)]PF_6$ (**7**)PF_6. The reaction of **1** or **6** with $SnCl_2$ resulted in cleavage of chloro and dithiocarbonate ligands, respectively, to give $CpRu(dppf)SnCl_3$ (**8**). All complexes were spectroscopically characterized and the structures of **2** and cationic complexes **4**–**7** were determined by single-crystal diffraction analyses.

Keywords: Ruthenium; 1,1′-Bis(diphenylphosphino)ferrocene; Sulfur-containing ligands; Cyclopentadienyl; Crystal structures

1. Introduction

There is continuing interest in the chemistry of transition-metal complexes with sulfur-containing ligands as model compounds for biological systems and industrial metal sulfide catalysts [1–5]. The chemistry of divalent ruthenium complexes $[CpRu(L)_2]^+$ containing phosphines and sulfur ligands has been extensively studied [6,7] but there are few examples of such complexes containing ferrocene ligands, such as 1,1′-bis(diphenylphosphino)ferrocene (dppf) [8–11]. Since dppf-containing complexes are of interest on account of their coordination versatility and catalytic potential [12,13], we have investigated the reactivity of CpRu(dppf)Cl (**1**) with some sulfur-based ligands. The results of this investigation are described herein.

2. Results and discussion

2.1. Reactions of CpRu(dppf)Cl (1)

2.1.1. With thiophenol

The reaction of **1** with thiophenol HSPh at room temperature gave air-stable orange precipitates of [CpRu(dppf)(SPh)] (**2**) in 83% yield (Scheme 1). The proton NMR spectrum of **2** shows the Cp ligand as a singlet at δ 3.96 and C_5H_4 in dppf as four equal-intensity singlets at δ 4.01, 4.23, 4.25 and 5.42; the $^{31}P\{^1H\}$ spectrum shows a resonance at δ 48.0 for the dppf ligand. The FAB^+-mass spectrum displays the parent ion at m/z 829, suggesting a mono-ruthenium complex, which is verified by its X-ray crystal structure described below. This neutral thiolate complex **2** is fairly stable towards oxidation by atmospheric oxygen, both in the solid state and in solution, and does not undergo dimerization or trimerization with loss of phosphine ligands, as observed by Shaver for the analogous compound $[CpRu(PPh_3)_2S(1\text{-}C_3H_7)]$ (Scheme 2) [14]. Undoubtedly, **2** owes its higher stability to the presence of the robust bidentate dppf chelate.

* Corresponding authors. Tel.: +65-68742677; fax: +65-67791691.
E-mail addresses: chmgohly@nus.edu.sg (L.Y. Goh), andyhor@nus.edu.sg (T.S.A. Hor).

0022-328X/$ - see front matter © 2004 Elsevier B.V. All rights reserved.
doi:10.1016/j.jorganchem.2003.12.020

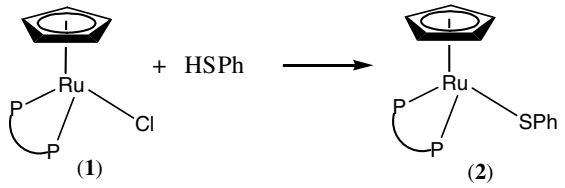

Scheme 1.

2.1.2. With 2-mercaptopyridine

The orange complex $[CpRu(dppf)(SC_5H_4NH)]BPh_4$ (**3**)BPh_4 was obtained in 80% yield from a reaction of **1** with 2-mercaptopyridine $C_5H_4N(SH)$ (Scheme 3). Its ^1H NMR spectrum shows an N–H proton at δ 9.66, indicative of mono-coordination of SNC_5H_5 via its S atom, as was previously observed for $[CpRu(PPh_3)_2(SNH(C_5H_4))]^+$ [7b]. The ν_{N-H} stretch is observed at 3758 cm^{-1} in its IR spectrum. Unfortunately, X-ray diffraction-quality crystals could not be obtained.

2.1.3. With thiourea and trithiocarbonates

Other sulfur-donors can be conveniently introduced through a direct ligand (chloride) substitution reaction. For example, complex **1** reacts with thiourea $SC(NH_2)_2$ in the presence of NH_4PF_6 to give 84% yield of $[CpRu(dppf)(SC(NH_2)_2]PF_6$ (**4**)PF_6 (yellow) or with the trithiocarbonates, $SCS(CH)_2S$ and $SCS(CH_2)_2S$, to give $[CpRu(dppf)(SCS(CH)_2S]Cl$ (**5**)Cl (orange-red) and $[CpRu(dppf)(SCS(CH_2)_2S]Cl$ (**6**)Cl (orange-red), respectively, in 95% yields (Scheme 4).

In the ^1H NMR spectrum of complex $\mathbf{4}^+$, the proton resonance of Cp is observed as a singlet at δ 4.45 and of C_5H_4 in dppf as four singlets of equal-intensity at δ 4.13, 4.30, 4.38 and 4.87. The N–H proton is seen at δ 9.72. The $^{31}P\{^1H\}$ resonances are observed at δ 47.7 (dppf) and −144 (PF_6). In the IR spectrum, ν_{N-H} stretching frequencies are observed at 3382 and 3275 cm^{-1} and P–F stretching frequencies at 840 and 556 cm^{-1}. The

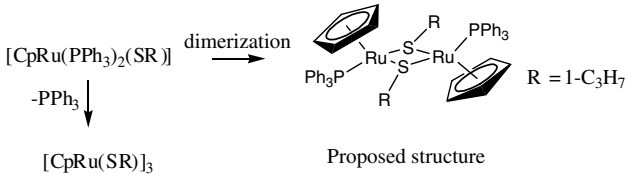

Scheme 2.

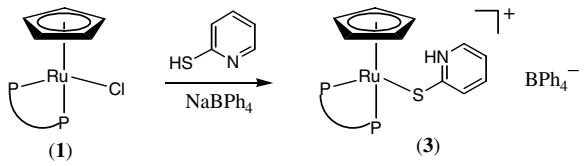

Scheme 3.

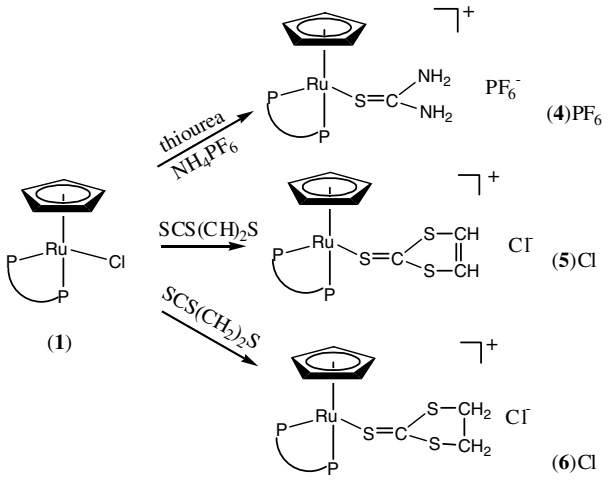

Scheme 4.

FAB$^+$-mass spectrum of **4** shows the parent ion at m/z 796, followed by a fragment m/z 721, indicating loss of the $SC(NH_2)_2$ ligand, while its FAB$^-$-mass spectrum shows the counter ion PF_6^- at m/z 145.

The ^1H NMR spectrum of $\mathbf{5}^+$ shows the CH resonances of trithiocarbonate ligand at δ 7.09–7.18 and δ 7.68–7.98, Cp as a singlet at δ 4.68 and C_5H_4 of dppf as four equal-intensity singlets at δ 4.14, 4.32, 4.40 and 4.75. The $^{31}P\{^1H\}$ resonance is seen at δ 48.5. The ^1H NMR spectrum of **6** shows a Cp peak at δ 4.15, CH_2 resonances as two singlets at δ 4.34 and 4.39, and C_5H_4 resonances of dppf as a broad apparent singlet at δ 4.68 at 300 MHz, and as overlapping singlets at δ 4.67 and 4.49 at 500 MHz. At this stage, we are unable to rationalize this difference from the normally observed four equal-intensity singlets for the α and β Cp protons of the ferrocenyl ligand, as observed in the other complexes in this work. The $^{31}P\{^1H\}$ resonance is seen at δ 49.6. The FAB$^+$-mass spectra of **5** and **6** show parent ions at m/z 855 and 857, respectively, and the fragment $[CpRu(dppf)]^+$ at m/z 721.

2.1.4. With $AuCl(SMe_2)$

Treatment of **1** with $AuCl(SMe_2)$ in the presence of NH_4PF_6 in acetone gave $[CpRu(dppf)(SMe_2)]PF_6$ (**7**)PF_6 in 70% yield (Scheme 5), together with the formation of NH_4AuCl_2. This finding is in agreement with the established lability of the thioether moiety in

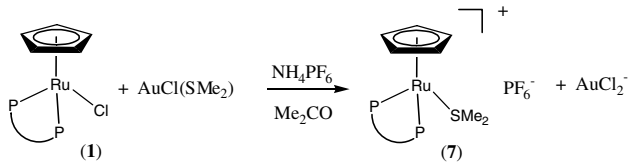

Scheme 5.

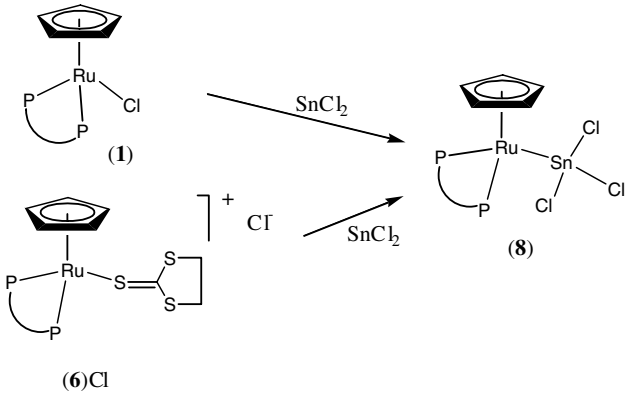

Scheme 6.

$AuCl(SMe_2)$; it is conceivable that the AuCl fragment could abstract chloride from **1** to form the $AuCl_2^-$ anion [15]. The NMR spectra of $\mathbf{7}^+$ show proton resonances of Me as a broad peak at δ 2.26 ($v_{1/2}$ ca. 91 Hz), Cp as a singlet at δ 4.79, C_5H_4 of dppf as four equal-intensity resonances at δ 4.72, 4.49, 4.32, 4.26 and ^{31}P resonances for dppf at δ 48.4, and a septet for PF_6 at δ −144. The FAB^+-mass spectrum shows the parent ion at m/z 783 and a fragment at 721 indicating the loss of the SMe_2 ligand. The FAB^--mass spectrum shows m/z 145 for the counter ion PF_6, the presence of which is also supported by ν_{P-F} stretching frequencies at 842 and 557 cm^{-1} in its IR spectrum.

2.1.5. With $SnCl_2$

Treatment of **1** with $SnCl_2$ gave $[CpRu(dppf)SnCl_3]$ (**8**) in 90% yield (Scheme 6). The FAB^+-mass spectrum shows the parent ion at m/z 945 $[M]^+$, and fragments indicating loss of $SnCl_2$ and $SnCl_3$ at 756 $[M-SnCl_2]^+$ and 721 $[M-SnCl_3]^+$, respectively. The NMR spectra show the Cp proton resonance at δ 4.68 and the C_5H_4 protons of dppf ligand as four equal-intensity singlets at δ 5.16, 4.38, 4.36 and 4.27, and a sharp $^{31}P\{^1H\}$ resonance at δ 50.5. The Cp resonance was observed at δ 4.5 in the related compound $[CpRu(PPh_3)_2SnCl_3]$ prepared by Siebald and co-workers [16] from the reaction of $[CpRu(PPh_3)_2Cl]$ with $SnCl_2$. An in situ NMR spectral study showed that the reaction of **6** with $SnCl_2$ also gave $[CpRu(dppf)SnCl_3]$ (**8**) together with free trithiocarbonate ligand $SCS(CH_2)_2S$.

2.2. Molecular structures

The molecular structures of the **2**, **4**–**7** cations have been determined by single-crystal X-ray diffraction analyses, and are shown in Figs. 1–5; selected bond parameters of these complexes are summarized in Table 1.

The crystal structure of complex [CpRu(dppf)(SPh)] (**2**) contains two independent molecules in the asymmetric unit (Fig. 1(a)). The two independent molecules of **2** are not superimposable as may be seen from

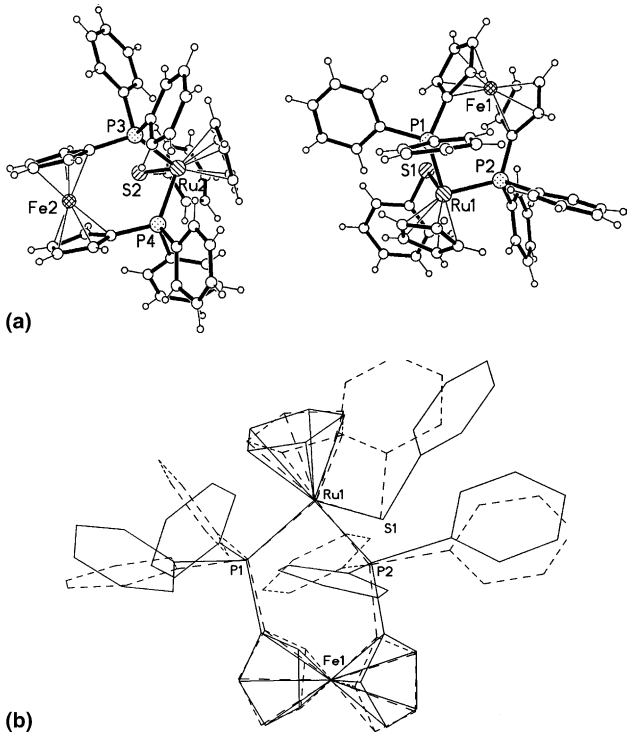

Fig. 1. (a) Molecular structures of the two independent molecules of [CpRu(dppf)(SPh)] (**2**). (b) Superimposition of the two independent molecules of (**2**).

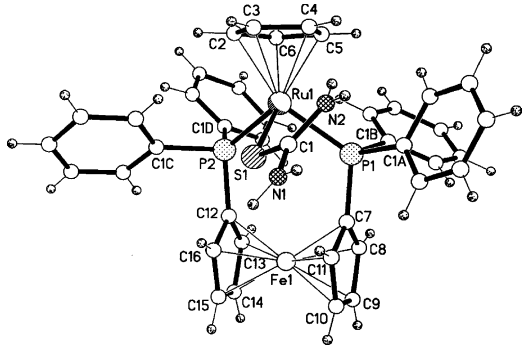

Fig. 2. Molecular structure of $[CpRu(dppf)(SC(NH_2)_2]^+$ (**4**).

Fig.1(b) which highlights the major differences in the orientations of the P- and S-bound phenyl groups and less major differences between the Cp rings in the two independent molecules. Consistent with this, there are no significant differences between the bond parameters of the two molecules. The Ru centre is coordinated by a Cp ring, that occupies one octahedral face, two P atoms of the diphosphine ligand and the thiolate S of the thiophenolate; the two P and S atoms define the second octahedral face. The Ru–S bond distances in **2** are 2.434(4) and 2.454(3) Å which are significantly longer than other examples of Ru(II)–S(thiolate) bonds, e.g., 2.30 Å (av.) in $[CpRu(S\text{-}1\text{-}C_3H_7)]_3$ [14], 2.3763(13)–2.3858(13)Å in $(arene)Ru(S(CH_2CH_2S)_2)$ [17] and

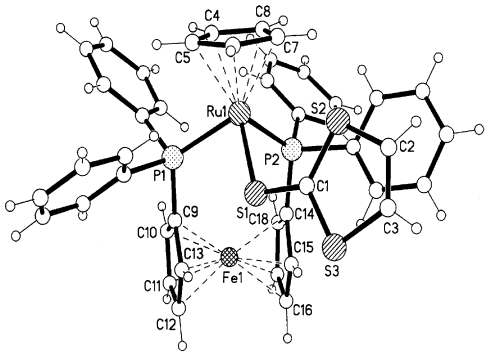

Fig. 3. Molecular structure of $[CpRu(dppf)(SCS(CH_2)_2S)]^+$ (**5**).

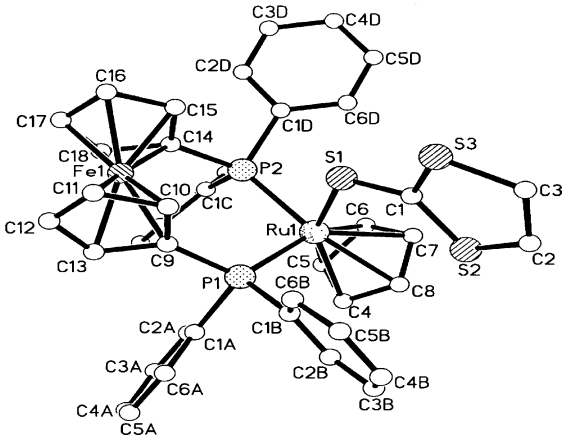

Fig. 4. Molecular structure of $[CpRu(dppf)(SCS(CH_2)_2S)]^+$ (**6**).

2.320(2)–2.4155(8)Å in similar thiolate/thioether complexes [18], as well as those in other sulfur-containing complexes described in this paper (seen in Table 1). The

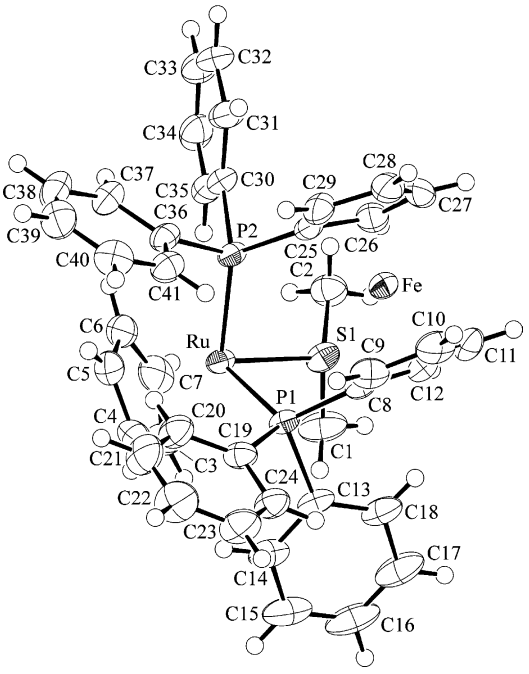

Fig. 5. Molecular structure of $[CpRu(dppf)(SMe_2)]^+$ (**7**).

long Ru–S bond is due to the destabilizing filled–filled dπ–pπ orbital interaction between the p-type sulfur lone pair and the formally occupied metal dπ orbitals of the Ru(II) low spin d_6-centre, as sustantiated by Fenske-Hall molecular orbital calculations coupled with gas-phase photoelectron spectroscopy for CpFe thiophenolate complexes by Ashby et al. [19].

A diffraction-quality crystal of **3** has not been obtained. Its formulation with a 1H-pyridinethione ligand as presented in Scheme 3, is consistent with the

Table 1
Selected bond lengths (Å) and bond angles (°) of complex **2**[a], and cations **4**–**7**

Complexes	Ru–P	Ru–S	C–S	P–Ru–P	P–Ru–S
[CpRu(dppf)(SPh)] (**2**)	2.284(3)[A] 2.302(3)[A] 2.295(3)[B] 2.306(3)[B]	2.434(4)[A] 2.454(3)[B]	1.779(8) 1.793(12)	99.02(10)[A] 98.52(10)[B]	89.29(11)[A] 85.75(12)[B]
$[CpRu(dppf)(SC(NH_2)_2]PF_6$ (**4**)PF_6	2.313(2); 2.309(2)	2.395(3)	1.719(11) C–N: 1.349(12) 1.315(12)	96.74(9)	88.64(9) 86.24(9)
$[CpRu(dppf)(SCS(CH)_2S]Cl$ (**5**)Cl	2.3076(14) 2.3156(13)	2.3863(13)	1.692(6) 1.695(7) 1.730(5)	97.35(5)	87.58(5) 86.72(5)
$[CpRu(dppf)(SCS(CH_2)_2S]PF_6$ (**6**)PF_6	2.3207(9) 2.3231(10)	2.3417(10)	1.659(4) 1.687(4) 1.728(4)	98.13(3)	85.96(4) 86.72(5)
$[CpRu(dppf)(SMe_2)]PF_6$ (**7**)PF_6	2.3271(10) 2.3149(9)	2.3605(11)	1.799(4) 1.802(4)	97.40(3)	84.66(3) 95.86(4)

[a] Contains two independent molecules A and B in the unit cell.

unipositive charge of the complex ion and in agreement with postulations of Puerta for analogous complexes containing monodentate phosphines [7b].

In complex **4**, which crystallizes with $0.25CH_2Cl_2$ and $0.5H_2O$ molecules in the asymmetric unit, the CpRu moiety is coordinated to a chelating dppf ligand and one S atom of the thiourea ligand, as shown in Fig. 2, so that the overall coordination geometry is the same as that found in **2**. The Ru–P and Ru–S distances are in the expected ranges [17,18,20].

The structures of cationic $[CpRu(dppf)(SCS(CH)_2S)]^+$ (**5**) and $[CpRu(dppf)(SCS(CH_2)_2S)]^+$ (**6**) are similar, containing the trithiocarbonate ligands, $SCS(CH)_2S$ and $SCS(CH_2)_2S$, respectively (Figs. 3 and 4). The unit cell of **5** contains disordered solvent molecules so that for each **5**(Cl), there are 0.5EtOH, 0.5MeOH and $0.5H_2O$; chloride is not disordered, but two 1/4 of water molecules were found near methanol. There is experimental evidence that the Ru–S bond distance in $\mathbf{5}^+$ is significantly longer than that in $\mathbf{6}^+$ and, conversely, there is an indication that the Ru–P bond distances in $\mathbf{5}^+$ are shorter than those in $\mathbf{6}^+$. An examination of the parameters associated with the S-containing ligands reveals a plausible explanation for this. Thus, the C–C bond length of 1.337(11) Å in $\mathbf{5}^+$ is consistent with significant double bond character in this bond. Also noteworthy is that the two formally single C–S bond distances in $\mathbf{5}^+$ are identical (C1–S1 1.692(6) Å and C1–S2 1.695(7) Å) indicative of substantial delocalization of π-electron density over the CS_3 entity, shown in Chart 1; this does not occur in $\mathbf{6}^+$ with a saturated C–C link (1.404(7) Å) between the endocyclic S atoms. The above results in the decreased donor-capability of S1 in $\mathbf{5}^+$, with a weakening of the Ru–S bond.

$[CpRu(dppf)(SMe_2)]PF_6$ (**7**) possesses an octahedral coordination geometry at the Ru atom as found for the other complex geometries described above; Fig. 5. The structure crystallizes with $0.25CH_2Cl_2$ and 0.5MeOH molecules per $\mathbf{7}(PF_6)$ entity. As can be noted from the data in Table 2, the Ru–S and Ru–P bond distances in the cation are entirely consistent with the geometric parameters reported for the complex cations previously described.

3. Experimental

All reactions were performed under dry nitrogen using Schlenk techniques. ^1H and $^{31}P\{^1H\}$ NMR spectra were recorded on a Bruker ACF300 or AMX500 FT NMR spectrometer, with chemical shifts referenced to residual non-deuterio solvent and external H_3PO_4, respectively. IR spectra were obtained with KBr pellet on a Perkin–Elmer 1600 spectrophotometer. Mass spectra were obtained on a Finnigan MAT95XL-T spectrometer. All elemental analyses were performed in-house, using a Perkin–Elmer Model Number Series II CHNS/O 2400 analyser.

$RuCl_3 \cdot 3H_2O$ and $AuCl(SMe_2)$ were obtained from Aldrich. PPh_3, dppf, thiophenol, 2-mercaptopyridine, vinylene trithiocarbonate, ethylene trithiocarbonate and thiourea were supplied by Merck. $[CpRu(PPh_3)_2Cl]$ [21] and [CpRu(dppf)Cl] [22] were synthesized as described. All solvents were freshly distilled from standard drying agents before use.

3.1. Reactions of [CpRu(dppf)Cl] (1)

3.1.1. With thiophenol HSPh

To a yellow suspension of **1** (0.055 g, 0.07 mmol) in EtOH (20 ml), HSPh (0.01 ml, 0.1 mmol) was added and the mixture was stirred for 1 h. The resultant orange suspension was filtered to collect an orange precipitate of [CpRu(dppf)(SPh)] (**2**), which was washed twice with EtOH (2×2 ml), followed by diethyl ether (2×2 ml) and dried in vacuo (0.050 g, 0.06 mmol, 83% yield). Anal. Calc. for $C_{45}H_{38}P_2SFeRu$: C, 65.1; H, 4.6; P, 7.5; S, 3.9. Found: C, 65.2; H, 4.5; P, 7.4; S, 3.8%. ^1H NMR ($CDCl_3$): δ 3.97 (s, 5H, C5H5), 4.01, 4.23, 4.25 and 5.42 (each s, 2H, C5H4), and for Ph protons δ 6.84 (c.m., 2H), 6.93 (c.m., 2H), 7.24–7.40 (m, 17H) and 7.80 (c.m., 4H); ^{31}P $\{^1H\}$: δ 48.0. FAB$^+$-MS: m/z 829 $[M]^+$, 721 $[M-SPh]^+$. IR(KBr, cm^{-1}): ν 3048w, 2967w, 1573w, 1477w, 1433m, 1262m, 1157wsh, 1089vs, 1029vs, 802vs, 745s, 695vs, 626w, 546wsh, 502s, 475s and 440m.

3.1.2. With 2-mercaptopyridine (C_5H_4N)SH

To a yellow suspension of **1** (0.030 g, 0.04 mmol) in MeOH (20 ml) was added 2-mercatopyridine (0.006 g,

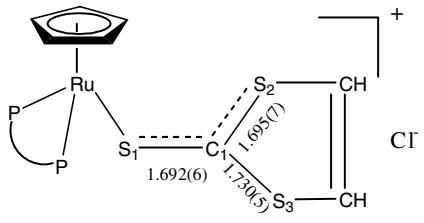

(**5**)

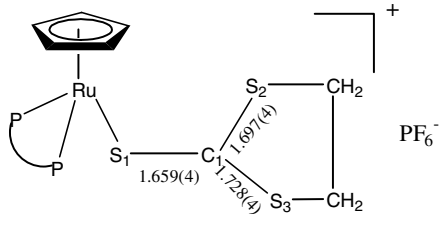

(**6**)

Chart 1.

Table 2
Crystal and structure refinement data

Complexes	**2**	(**4**)$PF_6 \cdot 0.25CH_2Cl_2 \cdot 0.5H_2O$	(**5**)$Cl \cdot 0.5EtOH \cdot 0.5MeOH \cdot 0.5H_2O$	(**6**)PF_6	(**7**)$PF_6 \cdot 0.25CH_2Cl_2 \cdot 0.5MeOH$
Empirical formula	$C_{45}H_{38}FeP_2RuS$	$C_{40.25}H_{38.5}Cl_{0.5}F_6FeN_2O_{0.5}P_2RuS$	$C_{43.5}H_{41}ClFeO_{1.5}P_2RuS_3$	$C_{42}H_{37}F_6FeP_3RuS_3$	$C_{41.75}H_{41.5}Cl_{0.5}F_6FeO_{0.5}P_3RuS$
Formula weight	829.67	971.85	937.75	1001.73	964.86
Temperature (K)	293(2)	223(2)	293(2)	223(2)	223(2)
Crystal system	Monoclinic	Monoclinic	Triclinic	Orthorhombic	Monoclinic
Space group	$P2_1$	$P2_1/c$	$P\bar{1}$	$Pbca$	$P2_1/c$
a (Å)	10.6928(6)	15.7683(11)	11.6049(11)	15.8272(8)	10.1794(4)
b (Å)	32.9248(19)	14.5401(11)	13.3588(13)	18.7391(11)	30.3410(12)
c (Å)	11.2853(7)	20.0040(14)	14.2870(14)	27.5132(16)	14.0100(6)
α (°)	90	90	103.867(2)	90	90
β (°)	110.821(1)	112.570(2)	96.888(2)	90	97.431(1)
γ (°)	90	90	92.123(2)	90	90
V (Å^3)	3713.6(4)	4235.1(5)	2129.8(4)	8160.1(8)	4290.7(3)
Z	4	4	2	8	4
Density (g/cm^3)	1.44	1.524	1.462	1.631	1.494
Absorption efficient (mm^{-1})	0.972	0.952	1.014	1.056	0.938
$F(000)$	1696	1966	957	4048	1958
Crystal size (mm^3)	$0.28 \times 0.10 \times 0.10$	$0.14 \times 0.1 \times 0.06$	$0.24 \times 0.2 \times 0.16$	$0.34 \times 0.10 \times 0.08$	$0.13 \times 0.21 \times 0.23$
θ range for data collection (°)	1.93–30.01	1.78–25.00	1.77–25.00	1.48–28.28	1.6–30.0
Index ranges	$-15 \leqslant h \leqslant 14$, $-46 \leqslant k \leqslant 46$, $-9 \leqslant l \leqslant 15$	$-18 \leqslant h \leqslant 14$, $-17 \leqslant k \leqslant 16$, $-23 \leqslant l \leqslant 22$	$-10 \leqslant h \leqslant 13$, $-15 \leqslant k \leqslant 15$, $-16 \leqslant l \leqslant 15$	$-20 \leqslant h \leqslant -21$, $-24 \leqslant k \leqslant 24$, $-36 \leqslant l \leqslant 18$	$-14 \leqslant h \leqslant 14$, $-37 \leqslant k \leqslant 42$, $-17 \leqslant l \leqslant 19$
Reflections collected	30,068	24,379	11,828	58,991	35,653
Independent reflections	19,947	7453	7477	10,122	12,497
Maximum and minimum transmission	0.9303 and 0.7656	0.9391 and 0.8593	0.8733 and 0.7804	0.9230 and 0.7154	0.844 and 1
Data/restraints/parameters	19947/1/813	7453/171/485	7477/4/481	10122/0/505	8982/2/499
Goodness-of-fit on F^2[c]	1.013	1.018	1.057	1.041	0.83
Final R indices $[I > 2\sigma(1)]$[a,b]	$R_1 = 0.0646$, $wR_2 = 0.1312$	$R_1 = 0.0749$, $wR_2 = 0.1796$	$R_1 = 0.0519$, $wR_2 = 0.1397$	$R_1 = 0.0536$, $wR_2 = 0.1184$	$R_1 = 0.056$, $wR_2 = 0.144$
R indices (all data)	$R_1 = 0.1431$, $wR_2 = 0.1784$	$R_1 = 0.1371$, $wR_2 = 0.2057$	$R_1 = 0.0664$, $wR_2 = 0.1453$	$R_1 = 0.0830$, $wR_2 = 0.1311$	$R_1 = 0.081$, $wR_2 = 0.161$
Largest difference peak and hole (e Å^{-3})	1.366 and −0.690	1.124 and −0.996	1.191 and −0.531	0.837 and −0.451	1.23 and −0.39

[a] $R_1 = (\sum |F_o| - |F_c|) \sum |F_o|$.
[b] $wR_2 = [(\sum \omega |F_o| - |F_c|)^2 / \sum \omega |F_o|^2]^{1/2}$.
[c] $GoF = [(\sum \omega |F_o| - |F_c|)^2 / (N_{obs} - N_{param})]^{1/2}$.

0.05 mmol), followed by $NaBPh_4$ (0.041 g, 0.1 mmol) and the mixture was stirred for 15 min, leading to an orange red mixture which was evacuated to dryness. The residue was extracted with CH_2Cl_2 (5 × 2 ml) to remove residual sodium salts; concentration of the combined extracts to ca. 1 ml, followed by addition of hexane (2 ml), gave orange solids of [CpRu(dppf)(S(C_5H_4NH)] BPh_4 (**3**)BPh_4 (0.036 g, 0.03 mmol, 80% yield). Anal. Calc. for $C_{68}H_{58}BNP_2SFeRu0.5CH_2Cl_2$: C, 68.9; H, 5.0; N, 1.2; P, 5.2; S, 2.7. Found: C, 68.9; H, 5.1; N, 1.2; P, 5.2; S, 2.7%. ^1H NMR ($CDCl_3$): δ 4.41 (s, 5H, C_5H_5); 4.11, 4.27, 4.33 and 4.85 (each s, 2H, C_5H_4); 5.81 (t, 1H), 6.13 (t, 1H), 6.89 (q, 6H), 7.02 (t,7H), 7.10 (d, 1H), 7.27 (c.m, 8H) and 7.42 (c.m., 20H) (8Ph + C_5H_4); 9.66 (br, 1H, NH); ^{31}P {^1H}: δ 47.7(s, dppf). ESI$^+$-MS: m/z 831 $[M]^+$, 721 $[M - SC_5H_4NH]^+$. ESI$^-$-MS: m/z 319 $[BPh_4]^-$. IR(KBr, cm^{-1}): ν_{NH} 3758w; ν (others) 3053wbr, 2907vw, 2854vw, 1650w, 1565m, 1476w, 1427w, 1261w, 1122msh, 1089s, 1033m, 803m, 739m, 701s and 475s.

3.1.3. With thiourea, $SC(NH_2)_2$

A yellow suspension of **1** (0.062 g, 0.08 mmol) and NH_4PF_6 (0.029 mg, 0.18 mmol) in MeOH (25 ml) was stirred for 30 min, $NH_2C(S)NH_2$ (0.010 g, 0.13 mmol) was then added and stirring continued for 3 h. The resultant suspension was filtered to remove the white precipitates of ammonium salts. The filtrate was evacuated to dryness and extracted with CH_2Cl_2 (5 × 2 ml) to remove residual ammonium salts; concentration of the combined extracts to ca. 1 ml, followed by addition of hexane (3 ml), gave yellow crystals of [CpRu(dppf)($SC(NH_2)_2$)]PF_6 (**4**)PF_6 (0.065 g, 0.07 mmol, 84% yield) obtained after cooling for 30 min at 0 °C. Anal. Calc. for $C_{40}H_{37}F_6N_2P_3SFeRu \cdot 0.5CH_2Cl_2$: C, 49.4; H, 3.9; N,

2.9; P, 9.4; S, 3.3; F, 11.6. Found: C, 49.4; H, 3.8; N, 2.8; P, 9.9; S, 3.2; F, 11.8%. ^{1}H NMR ($CDCl_3$): δ 4.13, 4.30, 4.38 and 4.87 (each s, 2H, C_5H_4), 4.45 (s, 5H, C_5H_5), 7.25–7.50 (m, 20H, Ph), 5.9 (vbr, $v_{1/2}$ ca. 50 Hz, ca.4H, NH_2);^{31}P {^{1}H}: δ 47.7 (s, dppf); −144 (septet, J_{P-F} 710 Hz, PF_6). FAB$^+$-MS: m/z 796 $[M]^+$, 721 $[M-NH_2C(S)NH_2]^+$. FAB$^-$-MS: m/z 145 $[PF_6]^-$. IR(KBr, cm^{-1}): v_{NH} 3382vs and 3275s; v_{PF6} 840s and 556s; v (others) 3176s, 2683vw, 1616vs, 1471m, 1415vs, 1262vw, 1085s, 727m, 625m and 480vsbr.

3.1.4. With vinylene trithiocarbonate $SCS(CH)_2S$ and ethylene trithiocarbonate $SCS(CH_2)_2S$

To a yellow solution of **1** (0.055 g, 0.07 mmol) in MeOH (20 ml) and CH_2Cl_2 (10 ml), $SCS(CH)_2S$ (0.009 g, 0.07 mmol) was added; the mixture turned orange red immediately and was stirred for 30 min. Concentration of the solution to ca. 1 ml, followed by addition of hexane (2 ml), gave orange red solids of [CpRu(dppf)($SCS(CH)_2S$)]Cl (**5**)Cl (0.061 g, 0.068 mmol, 95% yield). Anal. Calc. for $C_{42}H_{35}ClP_2S_3FeRu\cdot 0.5(C_6H_{14})$: C, 57.9; H, 4.5; P, 6.6; S, 10.3. Found: C, 58.1; H, 4.4; P, 6.3; S, 10.2%. ^{1}H NMR ($CDCl_3$): δ 4.68 (s, 5H, C_5H_5), 4.14, 4.32, 4.40 and 4.75 (each s, 2H, C_5H_4), 7.09–7.18 and 7.68–7.98 (m, 2H, CH), 7.41–7.50 (m, 20H, Ph); ^{31}P {^{1}H}: δ 48.5 (s, dppf). FAB$^+$-MS: m/z 855 $[M]^+$, 721 $[M-SCS(CH)_2S]^+$. IR(KBr, cm^{-1}): v 2922s, 2853m, 1648w, 1519w, 1459w, 1260vw, 1089s, 1029s, 808w and 695w.

A similar reaction of **1** (0.055 g, 0.07 mmol) with $SCS(CH_2)_2S$ (0.010 g, 0.07 mmol) gave orange red solids of [CpRu(dppf)($SCS(CH_2)_2S$)]Cl (**6**)Cl (0.057 g, 0.066 mmol, 95% yield). Anal. Calc. for $C_{42}H_{37}ClP_2S_3FeRu\cdot CH_2Cl_2$: C, 52.9; H, 4.0; P, 6.3; S, 9.8. Found: C, 52.6; H, 4.2; P, 6.0; S, 9.9%. ^{1}H NMR ($CDCl_3$): δ 4.15 (s, 5H, C_5H_5), 4.34, 4.39 (each s, 2H, CH_2), 4.68 (apparent s (br. $v_{1/2}=10$ Hz), which at 500 MHz is seen as overlapping singlets at δ 4.67 and 4.69, total 8H, C_5H_4), 7.39–7.51 (m, 20H, Ph); ^{13}C: 45.5 (CH_2); 84.3, 75.2, 74.2, 72.0 and 68.8 (Cp and Cp of dppf); 124.7, 127.8, 128.3, 130.2, 130.4, 133.3, 133.6 and 138.7 (Ph); 154.9 ($C(S)S_2$). ^{31}P{^{1}H}: δ 49.6 (s, dppf). FAB$^+$-MS: 857 $[M]^+$, 721 $[M-SCS(CH_2)_2S]^+$. IR(KBr, cm^{-1}): v 2985vw, 1625vwsh, 1615vw, 1478vw, 1432m, 1384vw, 1155msh, 1122m, 1089m, 1047s, 910w, 837m, 814msh, 751s, 698vs, 624m, 544msh, 507vs, 473s and 438s.

6 was converted to its PF_6 salt for obtaining single crystals. To an orange red solution of **6** (0.010 g, 0.01 mmol) in MeOH (5 ml), NH_4PF_6 (0.002 g, 0.01 mmol) was added and the mixture was stirred for 10 min. The resultant suspension was filtered to remove the white precipitates of ammonium salts. Concentration of the filtrate to ca. 0.5 ml, followed by addition of ether (1 ml), gave orange red crystals of [CpRudppf($SCS(CH_2)_2S$)] PF_6 (**6**)PF_6.

3.1.5. With $AuCl(SMe_2)$

To a yellow suspension of **1** (0.020 g, 0.03 mmol) in acetone (20 ml), $AuCl(SMe_2)$ (0.010 g, 0.03 mmol) and NH_4PF_6 (0.010 g, 0.06 mmol) were added and the mixture was stirred for 10 h. The resultant brown yellow suspension was filtered, to remove a yellow solid, which is mainly insoluble. ^{1}H and ^{31}P{^{1}H} NMR spectra of an $CDCl_3$ extract of this solid showed the presence of unreacted **1**. Presumably the insoluble component is NH_4AuCl_2 [15]. Concentration of the filtrate to ca. 1 ml, followed by addition of diethyl ether (2 ml) gave brown solids of [CpRu(dppf)(SMe_2)]PF_6 (**7**) PF_6 (0.019 g, 70%). Anal. Calc. for $C_{41}H_{39}F_6P_3SFeRu$: C, 53.1; H, 4.2; P, 10.0; S, 3.5. Found: C, 53.0; H, 4.4; P, 9.8; S, 3.4%. ^{1}H NMR ($CDCl_3$): δ 2.26 ($v_{1/2}=91$ Hz, 6H, CH_3), 4.79 (s, 5H, C_5H_5), 4.26, 4.32, 4.49 and 4.72 (s, 2H, C_5H_4), 7.21–7.23 (m, 4H, Ph), 7.32 (t, $J=7$ Hz, 4H, Ph), 7.40–.47 (m, 12 H, Ph); ^{31}P {^{1}H}: δ 48.4 (s) and −144 (septet, $J_{PF}=710$ Hz). FAB$^+$-MS: m/z 783 $[M]^+$, 721 $[M-SMe_2]^+$. FAB$^-$-MS: m/z 145 $[PF_6]^-$. IR(KBr, cm^{-1}): v_{PF6} 842 and 557.

3.1.6. With $SnCl_2$

To a yellow solution of **1** (0.037 g, 0.05 mmol) in toluene (5 ml) and MeOH (5 ml), $SnCl_2$ (0.011 g, 0.06 mmol) was added and the mixture was stirred for 6 h. The yellow resultant solution was evacuated to dryness and extracted with toluene (3×2 ml). The combined extracts were concentrated to ca. 2 ml, hexane (2 ml) was added, giving yellow solids of [CpRu(dppf)($SnCl_3$)] (**8**) (0.041 g, 0.04 mmol, 90% yield). Anal. Calc. for $C_{39}H_{33}Cl_3P_2FeRuSn$: C, 49.5; H, 3.5; P, 6.6; Cl, 11.3. Found: C, 49.6; H, 3.6; P, 6.9; Cl, 10.9%. ^{1}H NMR ($CDCl_3$): δ 4.27, 4.36, 4.38 and 5.16 (each s, 2H, C_5H_4), 4.68 (s, 5H, C_5H_5), 7.37 and 7.42 (each, c.m., total 20H, Ph); ^{31}P {^{1}H}: δ 50.5 (s). FAB$^+$-MS: m/z 945 $[M]^+$, 756 $[M-SnCl_2]^+$, 721 $[M-SnCl_3]^+$. IR(KBr, cm^{-1}): v 2928w, 1631w, 1563vw, 1433w, 1262m, 1162wsh,, 1089s, 1033s, 808m, 743m, 698s and 475s.

^{1}H NMR spectral monitoring of a reaction of **6** (6 mg, 0.006 mmol) with $SnCl_2$ (1.2 mg, 0.006 mmol) in $CDCl_3$ (0.5 ml) showed that **8** was produced, together with free $SCS(CH)_2S$ (δ (CH) 7.10).

3.2. Structure determinations

Diffraction-quality single crystals were obtained from solutions at 0 °C as follows: **2** and (**4**)$PF_6\cdot 0.25\ CH_2Cl_2\cdot 0.5H_2O$ as orange and yellow prisms, respectively, from CH_2Cl_2-hexane after 2–3 h; (**5**) $Cl0\cdot 5EtOH\cdot 0.5MeOH\cdot 0.5H_2O$ as orange prisms from EtOH/MeOH-ether after 30 min, (**7**) $PF_6\cdot 0.25CH_2\ Cl_2\cdot 0.5MeOH$ as yellow-brown prisms from CH_2Cl_2-MeOH after 2–3 h. (**6**)PF_6 was obtained as orange red prisms from acetone–ether after 3 days at room temperature.

X-ray data for **2**, (**4**)$PF_6 \cdot 0.25CH_2Cl_2 \cdot 0.5H_2O$, (**5**)$Cl \cdot 0.5EtOH \cdot 0.5MeOH \cdot 0.5H_2O$, (**6**)$PF_6$ and (**7**) $PF_6 \cdot 0.25CH_2Cl_2 \cdot 0.5MeOH$ were collected on a Siemens SMART diffractometer, equipped with a CCD detector, using Mo Kα radiation. Data were corrected for Lorentz and polarization effects with the SMART [23] program, and for absorption effects with SADABS [24]. Structure solution (heavy-atom methods) and refinement (on F^2: anisotropic displacement parameters, H atoms in calculated positions, and a weighting scheme of the form $w = 1/[\sigma^2(F_o^2) + aP^2 + bP]$, where $P = (F_o^2 + 2F_c^2)/3$) were carried out with the SHELXTL suite of programs [25]. The lattice of (**7**) PF_6 was found to contain residual electron density peaks that were modeled as 0.25 of a CH_2Cl_2 molecule and 0.5 of a MeOH molecule. These atoms were refined isotropically and with constrained C–Cl bond distances in the former. Crystal data and refinement details are collected in Table 1.

4. Conclusion

Sulfur-bonded CpRu(II) complexes, [CpRu(dppf)SPh] (**2**) and [CpRu(dppf)(L)]$^+$X (X = BPh_4, L = SC_5H_4NH (**3**); X = PF_6, L = $SC(NH_2)_2$ (**4**); X = Cl, L = $SCS(CH_2)_2S$ (**6**); X = Cl, L = $SCS(CH)_2S$ (**5**)), were obtained from chloride substitution in [CpRu(dppf)Cl] (**1**). Likewise, [CpRu(dppf)(SMe_2)]PF_6 (**7**) and [CpRu(dppf)($SnCl_3$)] (**8**) were obtained from the reaction of **1** with AuCl(SMe_2) and $SnCl_2$, respectively.

5. Supplementary material

Crystallographic data for **2** and **4**–**7** have been deposited at the Cambridge Crystallographic Data Centre with deposition numbers 223100–223104, respectively. Copies of the information may be obtained free of charge from The Director, CCDC, 12 Union Road, Cambridge CB2 1EZ, UK (fax: +44-1223-336033; e-mail: deposit@ccdc.cam.ac.uk or http://www.ccdc.cam.ac.uk).

Acknowledgements

Support of the National University of Singapore in the form of Grant Nos. RP14300077112 and RP143000135112 to LYG and a research scholarship to XLL are gratefully acknowledged. The authors also thank Ms. G.K. Tan for technical assistance.

References

[1] R. Weber, R. Prins, R.A. van Santen (Eds.), Transition Metal Suphides, Chemistry and Catalysis; NATO ASI Series, vol. 60, Kluwer Academic Publishers, Dordrecht, 1998.
[2] E.I. Stiefel, K. Matsumoto (Eds.), Transition Metal Sulfur Chemistry – Biological and Industrial Significance, ACS Symposium Series, vol. 653, 1996.
[3] A. Mùller, B. Krebs (Eds.), Sulfur – Its Significance for Chemistry; for the Geo-, Bio- and Cosmosphere and Technology, Elsevier, Amsterdam, 1984.
[4] R.A. Sanchez-Delgado, J. Mol. Catal. 86 (1994) 287.
[5] J.J.R. Fraústo da Silva, R.J.P. Williams, The Biological Chemistry of the Element, second ed., Clarendon, Oxford, 2001, pp. 164–170.
[6] G. Wilkinson, F.G.A. Stone, E.W. Abel (Eds.), Comprehensive Organometallic Chemistry, 7, Pergamon Press, Oxford, England, 1995, pp. 522–530.
[7] (a) See for instance recent papers: W.A. Schenk, J. Bezler, Eur. J. Inorg. Chem. 5 (1998) 605;
(b) A. Coto, M.J. Tenorio, M.C. Puerta, P. Valerga, Organometallics 17 (1998) 4392;
(c) W.A. Schenk, N. Kuhnert, Z. Naturforsch. B 55 (2000) 527;
(d) A. Shaver, M. El-khateeb, A.M. Lebuis, J. Organomet. Chem. 622 (2001) 1;
(e) M. El-khateeb, B. Wolfsberger, W.A. Schenk, J. Organomet. Chem. 612 (2001) 14;
(f) I. Kovacs, A.M. Lebuis, A. Shaver, Organometallics 20 (2001) 35;
(g) N. Kuhnert, N. Burzlaff, E. Dombrowski, W.A. Schenk, Z. Naturforsch. B 57 (2002) 259.
[8] R.T. Hembre, J.S. McQueen, J. Am. Chem. Soc. 118 (1996) 798.
[9] I.-Y. Wu, J.T. Lin, J. Luo, S.-S. Sun, C.-S. Li, K.J. Lin, C. Tsai, C.-C. Hsu, J.-L. Lin, Organometallics 16 (1997) 2038.
[10] M. Sato, M. Asai, J. Organomet. Chem. 508 (1996) 121.
[11] G. Bandoli, A. Dolmella, Coord. Chem. Rev. 209 (2000) 161.
[12] K.-S. Tan, T.S.A. Hor, in: A. Togni (Ed.), Ferrocenes – Homogeneous Catalysis, Organic Synthesis and Material Science, VCH, Weinheim, 1995, p. 3.
[13] P.A. Robles-Dutenhefiner, E.M. Moura, G.J. Gama, H.G.L. Siebald, E.V. Gusevskaya, J. Mol. Catal. A 164 (2000) 39.
[14] A. Shaver, P.-V. Plouffe, D.C. Liles, E. Singleton, Inorg. Chem. 31 (1992) 997.
[15] G. Wilkinson, R.D. Gillard, J.A. McCleverty (Eds.), Comprehensive Coordination Chemistry, 5, Pergamon Press, Oxford, England, 1987, pp. 870–875, and references therein.
[16] E.M. Moura, H.G.L. Siebald, G.M. de Lima, Polyhedron 21 (2002) 2323.
[17] R.Y.C. Shin, M.A. Bennett, L.Y. Goh, W. Chen, D.C.R. Hockless, W.K. Weng, K. Mashima, A.C. Willis, Inorg. Chem. 42 (2003) 96.
[18] M.A. Bennett, L.Y. Goh, A.C. Willis, J. Am. Chem. Soc. 118 (1996) 4984.
[19] M.T. Ashby, J.H. Enemark, D.L. Lichtenberger, Inorg. Chem. 27 (1988) 191.
[20] J. Amarasekera, T.B. Rauchfuss, A.L. Rheingold, Inorg. Chem. 26 (1987) 2017.
[21] M.I. Bruce, C. Hamiester, A.G. Swincer, R.C. Wallis, Inorg. Synth. 21 (1982) 78.
[22] M.I. Bruce, I.R. Bulter, W.R. Cullen, G.A. Koustanonis, M.R. Snow, E.R.T. Tiekink, Aust. J. Chem. 41 (1988) 963.
[23] SMART and SAINT Software Reference Manuals, Version 5.0, Bruker AXS Inc., Madison, WI, 1998.
[24] G.M. Sheldrick, SADABS Software for Empirical Absorption Correction, University of Göttingen, Germany, 2000.
[25] SHELXTL Reference Manual, Version 5.1, Bruker AXS Inc., Madison, WI, 1998.